Modelling of non- transferred argon-nitrogen plasma arc and plasma jet

2010 J. Phys.: Conf. Ser. 208 012047

(http://iopscience.iop.org/1742-6596/208/1/012047)

Journal of Physics: Conference Series **208** (2010) 012047 doi:10.1088/1742-6596/208/1/012047

Modelling of non- transferred Argon-Nitrogen Plasma Arc and Plasma Jet

B Selvan[1], K Ramachandran[1], T K Thiyagarajan[2], K P Sreekumar[2] and P V Ananthapadmanabhan[2]

[1] School of Mechanical and Building Sciences, VIT University, Vellore-632 014, India
[2] Laser and Plasma Technology Division, BARC, Mumbai-400 085, India

E-mail: b_selvan@yahoo.co.in

Abstract. One of the challenging problems in the plasma spray technique is reproducibility of the coating quality. This problem is mainly associated with arc fluctuations, which affect the plasma jet temperature and velocity inside the plasma torch. In this study, three- dimensional numerical models are developed to study the behaviour of Ar-N_2 plasma arc inside a non-transferred torch and plasma jet. Ar-N_2 plasma arc is simulated for given arc current and gas flow rate. Different arc sizes, which correspond to given torch power, are predicted. A most feasible arc size, which corresponds to an actual physical situation of the arc inside the torch, is identified using thermodynamic principle of minimum entropy production for particular torch power. Predicted torch efficiency is comparable with measured one. Cathode and anode losses are reported. Predicted temperature and velocity profiles at the nozzle exit are used to simulate the plasma jet. Since plasma gas is mixed with cold air, plasma jet is diffused in the radial direction. Three-dimensional effect on plasma jet temperature and velocity is diminishes along the axial direction.

1. Introduction

Plasma spraying is one of the important thermal spraying techniques used by industries. It has been widely used to produce metal and ceramic coatings for wear, corrosion and thermal barrier etc. Recently plasma jets have also been applied to waste treatment and synthesis of new materials. However, the symptomatic behaviour of an arc inside the torch leads to fluctuation of arc voltage resulting in fluctuation of temperature and velocity in the plasma jet [1]. The growth of thermal plasma technology is restricted due to the lack of understanding of the behaviour of the arc and the turbulent plasma jet. In order to understand the arc physics inside the plasma torch, simulation of an arc using both two-dimensional [2-4] and three-dimensional [5-13] models has been carried out. Plasma jet characteristics have been extensively studied by axi-symmetric [14-21] and three-dimensional models [22-30].Since the two-dimensional models could not predict the realistic phenomenon, three-dimensional models of plasma jet and plasma-particles interaction have been published [22-30]. Dilute particle loading and two way interaction between plasma and particles have been considered in several models [14, 18, 19, 26-29].

In these models, the temperature and velocity profiles at the torch exit are either assumed from the effective power or obtained from measurements [26-29]. Since the arc attaches at the anode as a constricted spot, plasma flow has a three-dimensional effect both inside the torch and at the torch exit.

However this effect is not considered in many published models. The correct profiles of temperature and velocity at the nozzle exit are important to simulate the plasma jet. In the present study, the realistic temperature and velocity profiles at the torch exit are obtained from the simulation of an arc using three-dimensional model for the given power and gas flow rate and using the same, a turbulent plasma jet is simulated and three-dimensional effects on the plasma jet are studied.

2. Model Description

2.1 Plasma arc

By assuming plasma flow is steady, in local thermodynamic equilibrium (LTE), optically thin, laminar and incompressible, the present model is developed. The arc core radius (R_{arc}) is assumed as the radial distance along the cathode from the centreline to the point at which current density is zero whereas arc length (L_{arc}) is assumed as the axial distance from the cathode at which current density is zero to the centre point of the anode arc spot. Harmonic mean electrical conductivity between plasma and anode material is assumed at the cells adjacent to the anode wall. Based on the foregoing assumptions, a set of governing equations to simulate the plasma arc flow inside the DC non transferred arc plasma torch can be expressed in the simplified form as

$$\mathrm{div}(\rho\vec{V}\phi) - \mathrm{div}(\Gamma_\phi \mathrm{grad}\,\phi) = S_\phi \tag{1}$$

For each equation, the dependent variable/property (ϕ), diffusion coefficient (Γ_ϕ) and source term (S_ϕ) are tabulated in Table 1. The first and second terms in the left hand side of the equation (1), where ρ is mass density, represent the transport of ϕ by means of convection and diffusion respectively. In table 1, u, v, w, h, j, μ, Cp, λ, S_R , ∇P, Ax, Ay & Az,, μ_0, B, φ and σ are respectively x-velocity, y-velocity, z-velocity, enthalpy, current density, viscosity, specific heat capacity at constant pressure, thermal conductivity, volumetric radiation loss, pressure gradient, vector potential in x, y and z directions, magnetic permeability, magnetic field, electric potential and electrical conductivity. The source terms in the momentum equation are pressure gradient and an electromagnetic force and the same in energy equation are the joule heating and the net radiation loss. The plasma gas is a mixture of argon and nitrogen. The net radiation emission coefficients [34-35], thermodynamic and transport properties of the plasma gases are taken from [31].

Table 1. Dependent variable/property (ϕ), diffusion coefficient (Γ_ϕ) and source term (S_ϕ) for each equation to simulate the plasma arc.

Equation	ϕ	Γ_ϕ	S_ϕ
Continuity	*1*	*0*	0
Momentum	*u, v & w*	μ	$-\nabla P + \vec{j}\times\vec{B}$
Energy	*h*	λ/Cp	$(j^2/\sigma) - S_R$
Electric potential	φ	σ	0
Magnetic vector potential	A_x, A_y & A_z,	*1*	$-\mu_0\vec{j}$ $(\vec{B} = \vec{\nabla}\times\vec{A})$

The computational geometry of the plasma torch is shown in figure 1. It is generated with 1, 05,600 calculation points. Mesh is refined near wall region to enhance the accuracy in the heat transfer to the wall. The boundary conditions used in this model are shown in table 2.

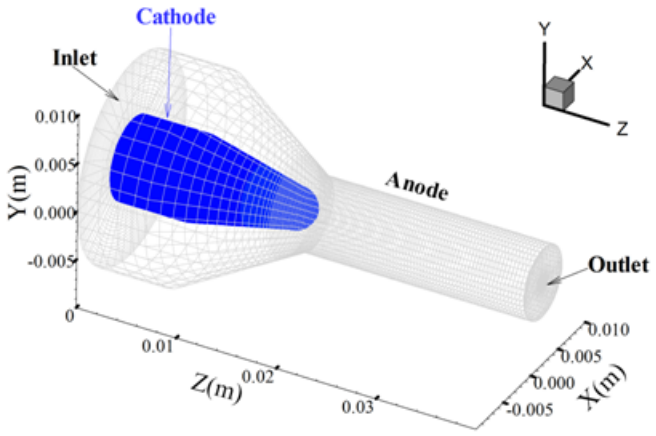

Figure 1. Computational geometry of the plasma torch

Table 2. Boundary conditions used in the plasma arc model

Boundary	Temperature	Velocity(V_i)	Elec. pot. (φ)	Mag. pot. (A_i)
Inlet	300 K	Mass flow rate (kg/s)	$\partial\varphi/\partial n=0$	$\partial A_i/\partial n=0$
Cathode	(T=3500 upto $r=R_{arc}$) $T(r)$	0.0	$j(r)$	$\partial A_i/\partial n=0$
Anode	$Q_a=h_{conv}(T_{wall}-T_{water})$	0.0	(φ =0 at spot) $\partial\varphi/\partial n=0$	$\partial A_i/\partial n=0$
Outlet	$\partial T/\partial n=0$	$\partial V_i/\partial n=0$	$\partial\varphi/\partial n=0$	0.0

The governing equations are solved by using FLUENT 6.3. The radial current density profile used at the cathode is assumed as

$$j(r)=j_{\max}\left[1-\left(\frac{r}{R_{arc}}\right)^{n}\right] \tag{2}$$

Where, r and n are radial distance from the torch axis and a parameter that specify the shape of the current density profile respectively. The j_{max} at the axis is fixed with certain value to ensure the integration of j(r) over the cathode equals to the applied current. The temperature at the cathode is 3500 K if the radial distance $r \le R_{arc}$ otherwise radial profile of the temperature along the cathode is given by

$$T(r) = 3200 \times \left[1 - \left(\frac{r - R_{arc}}{R_{\max} - R_{arc}} \right)^{n} \right] + 300 \tag{3}$$

Where, R_{max} and n are 4.0×10^{-3} m and 2.0 respectively. The size of the anode arc spot at the anode wall is assumed to be equal to the size of the arc core at the cathode. At the anode spot and wall, electric potential and gradient of electric potential are assumed to zero respectively. These boundary conditions make an arc current pass through anode spot only. Heat flux to the anode wall due to electron condensation, electron enthalpy transport and conductive heat transfer is given by [7,32,33].

$$Q_a = j\phi_w + \frac{5k_B}{2e} jT + S_R - \lambda \left. \frac{\partial T}{\partial r} \right|_{wall} = h_{conv}(T_{wall} - T_{water}) \tag{4}$$

Here ϕ_w, k_B, and e are the work function of the anode material, Boltzmann's constant and the electron charge respectively. Ion recombination is neglected since its contribution is about less than 5% of the total heat flux to the anode [32-33]. The radiation from the wall is also negligible since entire wall has a quite low temperature except arc spot. The convective heat transfer coefficient of cooling water h_{conv} is assumed as 2.0×10^5 W/m^2 K [7,8,12]. T_{wall} and T_{water} are respectively the local temperature of the wall and the temperature of the cooling water (300 K).

In the non-transferred arc, both arc length and arc core radius adjust themselves for same gas flow and arc current. A combination of arc core radius and arc length, which corresponds to the real size of the arc, is determined using the original principle of minimum entropy production, the formula used to calculate entropy production (Σ) in an arc channel is

$$\Sigma = \int_{A_{wall}} \frac{1}{T} \vec{J}_{th} \cdot d\vec{A} + \int_{A_{cross}} \frac{1}{T} \vec{J}_{th} \cdot d\vec{A} + \int_{A_{cross}} \frac{1}{T} \rho h \vec{V} \cdot d\vec{A} + \int_{V} \frac{\rho h}{T^2} (\vec{V} \cdot \vec{\nabla} T) dv \tag{5}$$

Details of the equation (2) can be found from the literature [12].

2.2 Plasma jet

The main assumptions used to simulate the plasma jet are the jet is steady, local thermodynamic equilibrium, optically thin, turbulent and incompressible, Ar-N_2 plasma jet is discharged into air at atmospheric pressure and effective species diffusivity is equal to thermal diffusivity. Table 3 shows an appropriate ϕ, Γ_ϕ and S_ϕ for continuity, momentum, energy and species equations which can be derived from equation (1). Standard K-ε model is used to account the turbulent characteristics of the plasma jet.

Table 3. Dependent variable/property (ϕ), diffusion coefficient (Γ_ϕ) and source term (S_ϕ) for each equation to simulate the plasma jet.

Equation	ϕ	Γ_ϕ	S_ϕ
Continuity	*1*	*0*	0
Momentum	*u, v & w*	$\mu_l+\mu_t$	$-\nabla P$
Energy	*h*	$\lambda/Cp+\mu_t/\mathrm{Pr}_t$	$-S_R$
Mass fraction	y_1 & y_2	$\lambda/Cp+\mu_t/\mathrm{Pr}_t$	0

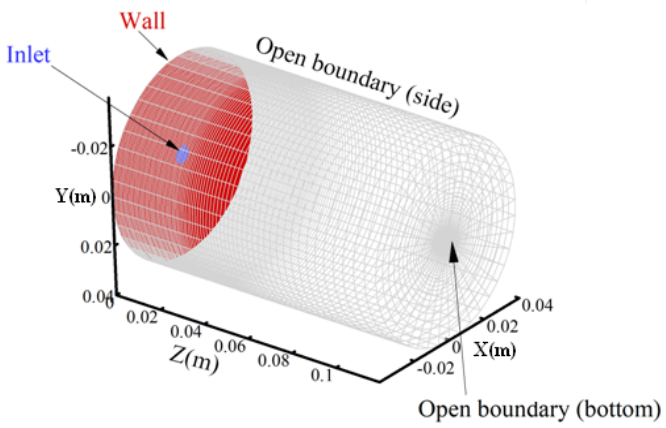

Figure 2. Computational geometry to simulate plasma jet.

Figure 2 shows the computational domain used to simulate the plasma jet. It is discretized in to 156240 calculation points. Mesh is refined in jet core region. The nozzle exit diameter is 7.0 mm at the top boundary and the remaining top boundary is anode wall. The temperature and velocity profiles at the nozzle exit are taken from the simulation results of plasma arc model explained in section 3. Atmospheric pressure is assumed at open boundaries. If the flow is reversed at these boundaries, atmospheric air is assumed to enter into the domain. If the flow is outward, gradient of all variables is zero other then pressure. The governing equations are solved by using FLUENT 6.3.

3. Results and discussion

3.1 Plasma arc

To simulate the plasma arc inside a torch, necessary input variables are gas flow rate and arc current and to validate the model, at least torch power and efficiency are needed. For the same, experiments are conducted for a gas flow rate of 20 slpm of Ar and 3 slpm of N_2 and current of 500A and torch power and efficiency are measured as 21.35 kW and 48.78 % respectively. In the present study, Ar-N_2 plasma arc is simulated using the gas flow rate and current used for the experiment. The variation of torch power with arc length is shown in figure 3 for various arc core radii.

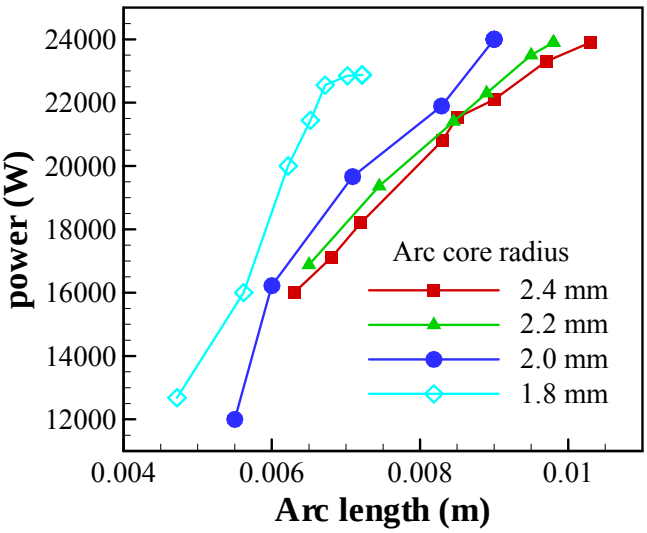

Figure 3. Effect of arc length on torch power for various arc core radii.

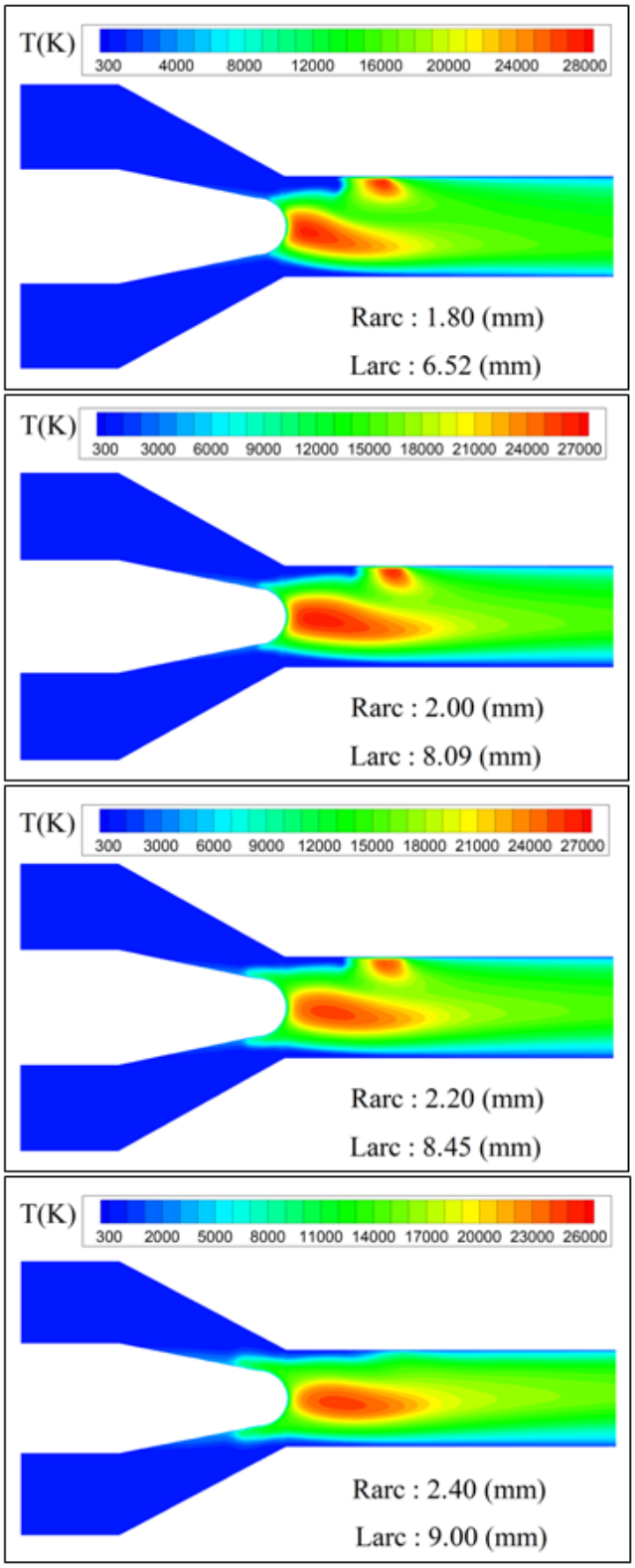

Figure 4. Four different temperature distributions inside the torch for 21.35 kW at given current and gas flow rate.

Torch power increases with increasing the arc length irrespective of arc core radius, whereas the same decreases with increasing the arc core radius. It is observed that different combinations of arc core radius and arc length produce the same torch power. Figure 4 shows the four different temperature distributions inside the torch for a torch power of 21.35 kW at above said current and gas flow rate. Since arc length is fixed in a transferred arc, arc radius adjusts itself to match a given power. But in non-transferred arc, both arc length and arc radius are not fixed. Since both arc length and arc radius adjust themselves for the power given to the torch, four combinations of arc core radius and arc length that generate same torch power at given current and gas flow rate are predicted. To find the most feasible combination of arc core radius and arc length that generate the measured power, an original principle of minimum entropy production is used. Using this principle, a combination of an arc core radius of 2 mm and an arc length of 8.09 mm is predicted as a most feasible one or as a real arc size for this case. Predicted cathode and anode losses, electro thermal efficiency, maximum temperature and velocity at the nozzle exit for the above said combination of arc length and arc radius are given in the table 4. Cathode and anode losses are as expected and electro thermal efficiency is comparable with measured one.

Table 4. Simulated results of Ar-N_2 plasma arc for the torch power of 21.35 kW

Current (A)	Ar (slpm)	N_2 (slpm)	Cathode loss (%)	Anode loss (%)	Efficiency (%)	Max. T_{exit} (K)	Max. V_{exit} (m/s)
500	20	3	9.6	44.1	46.30	15868	1026

3.2 Plasma jet

One of the important boundary conditions to simulate the plasma jet is nozzle exit temperature and velocity. These parameters are taken from the plasma arc model. Figure 5 (a) and (b) show the temperature and velocity contours of plasma jet. It is seen that both velocity and temperature are showing the non-symmetric nature very near to the nozzle exit. Peak temperature and velocity are not at the centre point. Diffusion of jet in the radial direction is clearly seen. Radial profiles of plasma jet temperature and velocity at various axial distances are shown in figure 6. Temperature and velocity at the nozzle exit clearly show the three-dimensional effect. This effect on both plasma jet temperature and velocity is similar. But the same on temperature is diminished faster than that on velocity along the axial direction. It can be concluded that particles behaviour would be almost same in the plasma jets simulated form both axis-symmetric and non-axis-symmetric boundary conditions at the nozzle exit, if particles are injected externally.

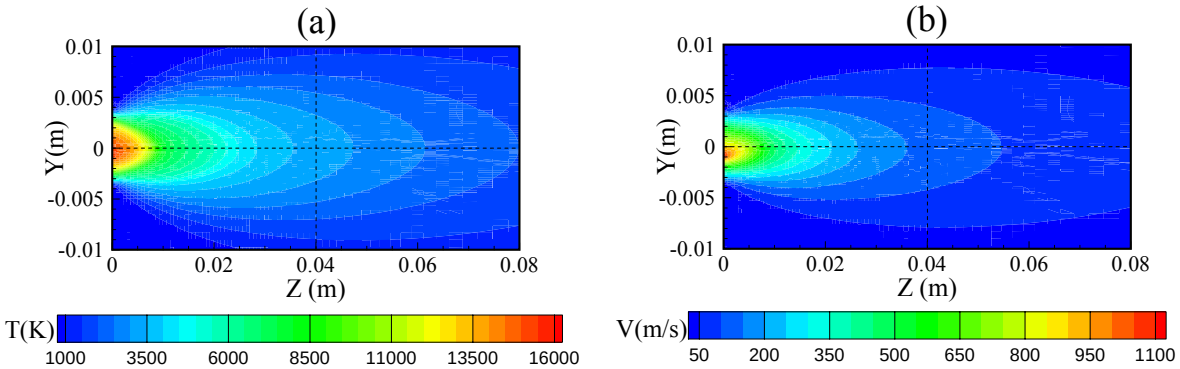

Figure 5. (a) Temperature and (b) Velocity contours of plasma jet.

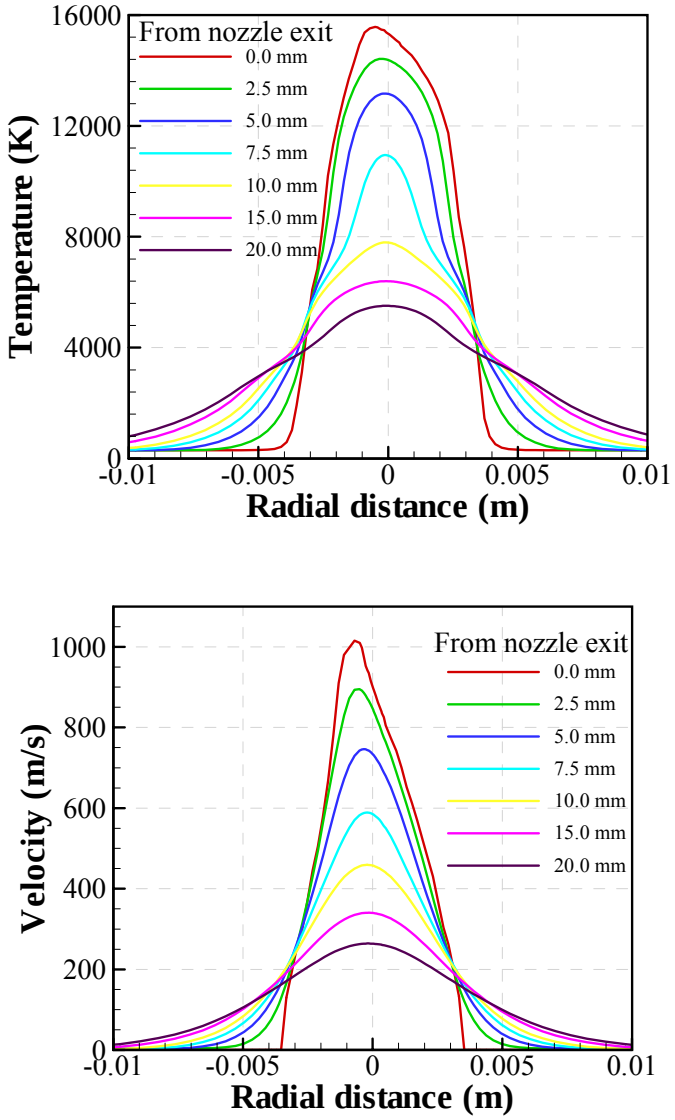

Figure 6. Radial profiles of temperature and velocity of the plasma jet at various axial distances

Centreline Ar, N_2 and air distributions are shown in figure 7. Since Ar-N_2 plasma gas is discharged from the nozzle exit, addition of Ar and N_2 mass fractions is 1.0. The plasma jet is mixed with cold air below the nozzle exit. Due to turbulent mixing, air is entered in the jet and jet is diffused in the radial direction. The Ar and N_2 mass fractions decrease along the axial distance due to effective mixing.

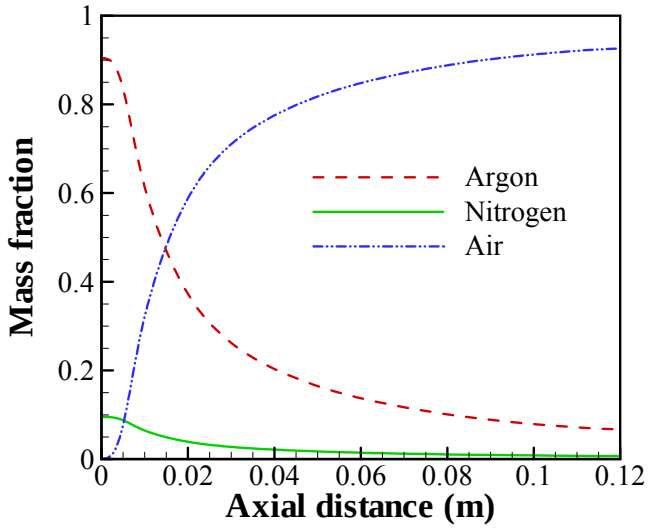

Figure 7. Centreline mass fraction of Ar, N_2 and air.

4. Conclusion

Ar-N_2 plasma arc and jet are simulated for given current and gas flow rate using two diffident three-dimensional computational fluid dynamics models. The following conclusions are derived from present study are

1. Arc length and arc radius adjust themselves to match the given torch power. Various combinations of arc core radius and arc length are predicted for the same power.
2. A feasible combination of arc length and arc radius is predicted using the principle of minimum entropy production.
3. Predicted efficiency is comparable with measured one and cathode and anode losses are as expected.
4. Three-dimensional effect on temperature is diminished faster than that on velocity along the axial direction
5. Mass fraction of Ar, N_2 and air at the centreline shows the effective mixing of plasma gas with an atmosphere.

5. References

[1] Duan Z and Heberlein J 2002 *J. Thermal Spray Technol.* **11** 44
[2] Westhoff R and Szekely J 1991 *J. Appl. Phys.* **70** 3455
[3] Paik S, Huang P C, Heberlein J and Pfender E 1993 *Plasma chem. Plasma Process.* **13** 379
[4] Murphy A B and Kovitya P 1993 *J. Appl. Phys.* **73** 4759
[5] Gonzalez J J, Freton P and Gleizes A 2002 *J. Phys. D: Appl. Phys.* **35** 3181
[6] Park J, heberlein J, Pfender E, Candler G and Chang C H 2008 *Plasma Chem. Plasma Process.* **28** 213
[7] Li H P, Pfender E and Chen X 2003 J. *Phys. D: Appl. Phys.* **36** 1084
[8] Baudry C, Vardelle A and Mariaux G 2005 *High Technology Plasma Processes* **9** 1
[9] Moreau E, Chazelas C, Mariaux G and Vardelle A 2006 J. *Thermal Spray Technol.* **15** 524
[10] Trelles J P and Heberlein J V R 2006 *J. Thermal Spray Technol*. **15** 563
[11] Chazelas C, Moreau E, Mariaux G and Vardelle A 2006 *High Temp. Material Processes* **10** 393
[12] Ramachandran K, Marquès J L, Vaßen R and Stöver D 2006 *J.Phys. D: Appl.*

Phys. **39** 3323
[13] Trelles J P, Pfender E and Heberlein J V R 2007 *J. Phys. D: Appl. Phys*. **40** 5635
[14] Lee Y C and Pfender E 1987 *Plasma Chem. Plasma Process.* **7** 1
[15] Delawari A H, Szekely J and Westhoff R 1990 *Plasma Chem. Plasma Process* **10** 501
[16] Sobelov V V, Guilemany J M and Martin A J 1999 *J. Mater. Process. Technol.* **87** 37
[17] Wan Y P, Prasad V, Wang G, Sampath S and Finke J R 1999 *ASME J. Heat Transfer* **121** 691
[18] Vardelle A, Vardelle M, Fauchais P, Proulx P and Boulos M I 1992 *Proc. Int. Conf. on Thermal Spray & Exposition* (Orlando, USA) p 543
[19] Bauchire J M, Gonzalez J J and Proulx P 1999 *J. Phys. D: Appl. Phys*.**32** 675
[20] Williamson R L, Finke J R and Chang C H 2000 *Plasma Chem.Plasma Process*. **20** 299
[21] Wan Y P, Gupta V, Deng Q, Sampath S, Prasad V, Williamson R and Finke J R 2001 *J. Thermal Spray Technol*. **10** 382
[22] Vardelle A, Fauchais P, Dussoubs B and Themelis N J 1998 *Plasma Chem. Plasma Process*. **18** 551
[23] Ahmed I and Bergman T.L 2000 *J. Thermal Spray Technol*. **9** 215
[24] Ahmed I and Bergman T L 2001 *ASME J. Heat Transfer* **123** 188
[25] Li H P and Chen X 2001 *Thin Solid Films* **390** 175
[26] Dussoubs B, Vardelle A, Mariaux G, Themelis N J and Fauchais P 2001 *J. Thermal Spray Technol.* **10** 105
[27] Vardelle M, Vardelle A, Fauchais P, Li K I, Dussoubs B and Themelis N J 2001 *J.Thermal Spray Technol*. **10** 267
[28] Mariaux G, Fauchais P, Vardelle A and Pateyron B 2001 *High Temp. Mater. Process* **5** 61
[29] Ramachandran K and Nishiyama H 2002 *J. Phys. D: Appl. Phys*. **35** 307
[30] Li H P and Chen X 2002 Plasma *Chem. Plasma Process*. **22** 27
[31] Murphy A B and Arundell C J 1994 *Plasma Chem. Plasma Process*. **14** 451
[32] Amakawa T, Jenista J, Heberlein J V R and Pfender E 1998 *J. Phys. D: Appl. Phys*. **31** 2826
[33] Jenista J, Heberlein J V R and Pfender E 1997 *IEEE Trans. Plasma Sci*. **25** 883
[34] Evans D L and Tankin R S 1967 *Phys. Fluids* **10** 1137-1144
[35] NASA -Technical Note D-4042

Acknowledgment
The research grand provided by BRNS, Department of Atomic Energy, Mumbai, India for this study is acknowledged.